Cationic Telechelic Polyelectrolytes: Synthesis by Group Transfer Polymerization and Self-Organization in Aqueous Media

George T. Gotzamanis,[†] Constantinos Tsitsilianis,*[,†] Stella C. Hadjiyannakou,[‡] Costas S. Patrickios,[‡] Robert Lupitskyy,[§] and Sergiy Minko[§]

Department of Chemical Engineering, University of Patras, 26504 Patras, Greece, and Institute of Chemical Engineering and High-Temperature Chemical Processes, FORTH/ICE-HT; Department of Chemistry, University of Cyprus, P.O. Box 20537, 1678 Nicosia, Cyprus; and Department of Chemistry, Clarkson University, Potsdam, New York 13699-5810

Received July 21, 2005; Revised Manuscript Received November 23, 2005

ABSTRACT: ABA triblock copolymers comprising a relative long poly(2-(dimethylamino)ethyl methacrylate) end-capped by short poly(methyl methacrylate) blocks (PMMA-*b*-PDMAEMA-*b*-PMMA) were synthesized using group transfer polymerization (GTP), and their aqueous solution properties were explored in aqueous media. At low pH these copolymers behaved as cationic telechelic polyelectrolytes (TP) and were self-organized through hydrophobic interactions among the PMMA blocks (stickers). Two types of associates were observed by atomic force microscopy (AFM) at very low concentrations: end-to-end linear associates and star like "hairy" loose aggregates where the one end of the TP was located in an irregular hydrophobic core and the other remained as a dangling end (absence of looping chains). By increasing the concentration, finite size clusters (microgels) were formed, the size of which changed continuously, leading eventually to the formation of an infinite transient network. All the structures were visualized by AFM with molecular resolution.

Introduction

Water-soluble polymers bearing hydrophobic groups (stickers), either at the end of the hydrophilic chain (block copolymers of the ABA type) or grafted as pendant groups along the chain, are known as associative polymers (APs).[1−3] When dissolved in aqueous media, these copolymers self-associate into micelles and in a second level of hierarchy, in transient networks, and find application in the industries of cosmetics and coatings as rheology modifiers, in molecular separator systems, and as suspending agents.[4]

Telechelic polyelectrolytes (TPs) represent a novel class of AP, constituted from a long polyelectrolyte chain end-capped by short hydrophobic polymeric chains. Polystyrene-*b*-poly(acrylic acid)-*b*-polystyrene was the first example of such AP, exhibiting unique properties in alkaline aqueous solutions (high pH). The main feature distinguishing TPs from conventional telechelic APs (nonionic hydrophilic part) is that the chain conformation of the soluble part can be controlled by external conditions such as the pH and the ionic strength. At a certain pH (depending on polyelectrolyte nature) and under salt-free conditions, the central chain adopts a stretched conformation, which has fundamental consequences on TP association and rheological properties.[5−8]

A number of recent studies concern block copolymers bearing the ionizable hydrophilic 2-(dimethylamino)ethyl methacrylate (DMAEMA) and/or its diethyl homologue (DEAEMA) as one of the blocks. PDMAEMA-containing block copolymers include amphiphilic block copolymers PDMAEMA−PMMA,[9] double-hydrophilic diblock copolymers P2VP-*b*-PDMAEMA,[10] and/or PDMAEMA-*b*-PDEAEMA[11] with interesting responsive micellar properties, PMMA−PDMAEMA−PMMA model chemically cross-linked gels,[12,13] and finally biocompatible macromolecules capable of transferring genetic materials to cells.[14] At low pH, PDMAEMA is protonated and transformed to a positively charged polyelectrolyte, like poly(2-vinylpyridine) (P2VP). However, unlike P2VP, which is water-insoluble above pH 5, PDMAEMA is water-soluble over the whole pH range, and it is partially protonated in the range of physiological pH (7.2). Therefore, this homopolymer is a nice candidate for macromolecular engineering of polymers suitable for biomedical applications such as carriers of nucleic acid[15] and/or DNA.[14]

In this work, cationic TP comprising a relative long PDMAEMA block end-capped by short PMMA blocks have been synthesized and explored in aqueous media. The motivation for this work was twofold: (a) from the synthetic point of view to synthesize telechelic polyelectrolytes by a less demanding "living" polymerization method such as GTP that proceeds at room temperature and (b) from the potential application point of view to combine the excellent properties of telechelic polyelectrolyte physical gels with the benefits of biocompatibility and capability of cationic macromolecules to be complexed with DNA.

Experimental Section

Materials. All reagents were purchased from Aldrich, Germany, unless stated otherwise. Two monomers were used for the synthesis of the polymers: the hydrophobic methyl methacrylate (MMA, 99%) and the hydrophilic 2-(dimethylamino)ethyl methacrylate (DMAEMA, 98%). The bifunctional GTP initiator, 1,4-bis(methoxytrimethylsiloxymethylene)cyclohexane (MTSCH), was used. This was prepared by the silylation of dimethyl 1,4-cyclohexanedicarboxylate (97%), performed in two steps in absolute tetrahydrofuran (THF): first, the reaction of dimethyl 1,4-cyclohexanedicarboxylate by *n*-butyllithium (2.5 M in hexanes) and diisopropylamine (95%) at −78 °C for 2 h; second, the reaction of the product of the first reaction with trimethylsilyl chloride (95%) at 0 °C for 2 h.

Tetrabutylammonium bibenzoate (TBABB) served as the catalyst of the polymerization. This was prepared by the reaction of tetrabutylammonium hydroxide (40% aqueous solution) with ben-

* To whom correspondence should be addressed: e-mail ct@chemeng.upatras.gr, Fax +30 2610 997266.
† University of Patras.
‡ University of Cyprus.
§ Clarkson University.

10.1021/ma051592e CCC: $33.50
Published on Web 12/22/2005

zoic acid (99%), following the method of Dicker et al.[19] TBABB was stored under vacuum until the time of polymer synthesis. THF was the polymerization solvent, which was dried by refluxing it for 3 days over a potassium/sodium alloy, and was freshly distilled prior to use.

Methods. MMA and DMAEMA were passed through basic alumina columns to remove the polymerization inhibitor and protic impurities. Both monomers were stirred overnight over calcium hydride and an added free radical inhibitor, 2,2-diphenyl-1-picrylhydrazyl hydrate (DPPH). Calcium hydride neutralizes the last traces of moisture and protic impurities, whereas DPPH prevents undesired free radical polymerization. The two monomers were subsequently stored in the refrigerator. MMA, DMAEMA, and MTSCH were vacuum-distilled and stored in the refrigerator in graduated Schlenk flasks under a nitrogen atmosphere until use.

Polymer Synthesis. The polymerization reactions were carried out under a dry nitrogen atmosphere. All glassware was dried in an oven at 140 °C, and all transfers of liquid were performed using glass syringes. All block copolymers were prepared by sequential monomer addition. The procedure followed to synthesize the MMA_{32}-*b*-$DMAEMA_{224}$-*b*-MMA_{32} triblock copolymer with a DMAEMA/MMA theoretical molar ratio 80/20 is described below. A 250 mL three-neck round-bottom flask, containing a small amount of TBABB catalyst, was fitted with two dropping funnels and a rubber septum. To this flask, 50 mL of freshly distilled THF was syringed through the septum, followed by 0.50 mL of MTSCH (0.60 g, 1.7×10^{-3} mol) bifunctional initiator. Subsequently, 40.3 mL of the first monomer, DMAEMA (37.6 g, 0.24 mol), was introduced to the reactor via one of the dropping funnels at a rate of 6−7 mL/min. This resulted in an exotherm from 26.2 to 47.0 °C. When the exotherm abated, samples of the resulting DMAEMA homopolymer were extracted for gel permeation chromatography (GPC) and proton nuclear magnetic resonance (^{1}H NMR) spectroscopy analyses. Then, 6.4 mL of the second monomer, MMA (6.0 g, 0.06 mol), was slowly introduced to the reactor via the other dropping funnel, resulting in an exotherm from 31.2 to 37.0 °C. Finally, samples for GPC and ^{1}H NMR were obtained.

All the other triblock copolymers were synthesized similarly, by changing the monomer feed ratio to achieve the different copolymer compositions.

Characterization in Organic Solvents. Molecular weights (MWs) and molecular weight distributions (MWDs) were determined using GPC. The GPC equipment consisted of a PL-LC1120 isocratic pump, an ERC-7515A refractive index detector (Polymer Laboratories), and a PL mixed "D" column. Calibration was carried out using seven PMMA standards with M_ws 630, 4250, 13 000, 28 000, 50 000, 128 000, and 260 000 g mol^{-1}. The eluent (THF) was delivered at a flow rate of 1 mL min^{-1}. The ^{1}H NMR spectra of polymer solutions in deuterated chloroform were recorded using a 300 MHz Avance Bruker spectrometer equipped with an Ultrashield magnet.

Hydrogen Ion Titration. 5 g of 0.1% w/w solutions of each polymer was titrated between pH 2 and 12 using a standard NaOH 0.5 M solution under continuous stirring. The pH was measured using a Corning PS30 portable pH meter. The effective p*K*s were calculated as the pH at 50% ionization.

Static Light Scattering. The static light scattering (SLS) experiments were carried out using a thermally regulated (±0.1 °C) spectrogoniometer model SEM RD (Sematech, France) equipped with a He−Ne laser (632.8 nm). The refractive index increments d*n*/d*c* required for the SLS measurements were obtained by means of a Chromatic KMX-16 differential refractometer operating at 632.8 nm.

Dynamic Light Scattering. Autocorrelation functions $g(q,t)$ were measured with a full multiple digital correlator (ALV-5000/FAST) equipped with 280 channels. The light source was an argon ion laser (Spectra Physics 2020) operating in single mode at 488 nm with a constant output power of about 150 mW. The correlation functions were analyzed by the constrained regularized CONTIN method through CoVA-Jacek Gapinski 2001 software. The apparent diffusion coefficients, $D_{app} = \Gamma/q^2$ ($q = (4\pi n/\lambda)\sin(\theta/2)$, n is the refractive index of the solvent), were determined at the peak of the decay rate distributions and the apparent hydrodynamic radii via the Stokes−Einstein equation:

$$R_{h,app} = k_B T/(6\pi\eta D_{app})$$

where k_B is the Boltzmann constant and η is the viscosity of the solvent at temperature T.

Atomic Force Microscopy. AFM images were recorded using a DI multimode scanning probe microscope (Veeco Instruments Inc., Woodbury, NY) operating in the tapping mode. Silicon tip budget sensors (Innovative Solutions Bulgaria, Sofia, Bulgaria) with a radius of <10 nm, a spring constant of 40 N/m, and a resonance frequency of 250−300 kHz were used. AFM images were recorded in 1 s^{-1} (1 Hz) at 512 pixel resolution and ∼1.7 V amplitude set point. Mica of V-1 grade (Structure Probe, Inc., West Chester, PA) was used as substrate (disks of 12 mm diameter, freshly cleaved before each spin-coating).

Sample Preparation. For the static and dynamic light scattering experiments the most concentrated sample solutions were directly prepared to the final desired concentration. The proper amount of polymer was weighed in a screw-capped vial. First, an equivalent amount of HCl (1 or 0.1 N) was added to ionize the tertiary amine groups of the PDMAEMA block, and then triply distilled water (Millipore) was added to the final volume. The resulting solution had a pH of 3. Samples of lower C_p were obtained by the appropriate dilution of the more concentrated solutions with aqueous HCl solution of pH 3 and equilibration at room temperature for several hours. For the rheological experiments the solutions were directly prepared to the final desired concentration following the same procedure.

Samples for AFM Experiments at Low Polymer Concentration (0.0001%). A drop of polymer solution was deposited on the mica surface. After 5 min contact with the substrate the drop was removed by centrifugal force (using a spin-coater). The 5 min contact was optimized to collect some amount of the polymer molecules adsorbed on the surface. We assumed that a strong interaction of the polymer with the solid substrate may modify conformations of the polymer chains and destroy micelles. However, the preadsorbed polymer will decrease the interaction of micelles with the substrate to a level when rapidly deposited micelles during the spin-casting step will not be destroyed by adsorption forces.

Samples for AFM Experiments at High Polymer Concentration (0.25%). A drop of polymer solution was deposited onto the mica surface from a syringe. Afterward, the sample was immediately rinsed with Millipore water to remove the polymer solution. Then the sample was dried by centrifugal forces on the spin-coater.

Rheometry. The rheological measurements were carried out using a controlled strain rheometer ARES Rheometric Scientific, equipped with either a cone−plate geometry (diameter 25 mm, cone angle 5,7°, truncation 56 μm) or a Couette geometry (gap 1,1 mm) depending on the viscosity of the solutions. Care to prevent solvent evaporation was undertaken. After each sample loading, a delay of 5 min was applied before measurements to erase the mechanical history. The temperature, fixed at 25 ± 0.1 °C, was controlled by a water bath circulator.

Results and Discussion

Polymer Synthesis and Characterization. Four PMMA−PDMAEMA−PMMA triblock copolymers of different composition (5, 10, 20, and 30% mol MMA) and approximately the same MW were synthesized by GTP using a bifunctional initiator. The designed MWs were rather large and close to the limits of the GTP method, to ensure the desired rheological properties. The number-average molecular weigths, M_n, were found greater than the theoretical values, reflecting partial initiator deactivation due to the low initiator concentration. The polydispersity indices (M_w/M_n) ranged between 1.26 and 1.52. The composition in MMA of the copolymers as determined by

Table 1. Molecular Characteristics of PMMA-*b*-PDMAEMA-*b*-PMMA Copolymers

polymer type	M_n[a]	M_w	M_w/M_n[a]	mol % MMA	wt % MMA	p*K*	precipitation pH
$DMAEMA_{196}$	31 700	48 200[a]	1.52				
MMA_2-*b*-$DMAEMA_{196}$-*b*-MMA_2		48 600[b]	1.48	2	1.3	7.3	10.78
$DMAEMA_{252}$	38 000	52 000[a]	1.37				
MMA_{16}-*b*-$DMAEMA_{252}$-*b*-MMA_{16}		55 200[b]	1.48	11.6	8.0	7.2	10.78
$DMAEMA_{224}$	30 800	36 700[a]	1.19				
MMA_{32}-*b*-$DMAEMA_{224}$-*b*-MMA_{32}		43 100[b]	1.26	22.3	18.1	7.0	10.86
$DMAEMA_{180}$	26 800	35 100[a]	1.31				
MMA_{35}-*b*-$DMAEMA_{180}$-*b*-MMA_{35}		42 100[b]	1.46	28.6	24.6	7.3	9.89

[a] Measured by SEC chromatography. [b] Calculated from the ^{1}H NMR results.

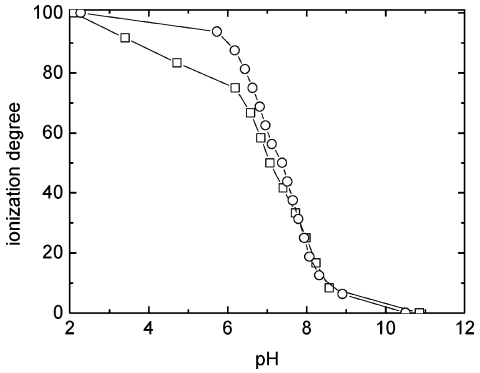

Figure 1. Hydrogen ion titration curves for the MMA_{32}−$DMAEMA_{224}$−MMA_{32} triblock copolymer (□) and the $DMAEMA_{224}$ homopolymer (○) in water and 25 °C.

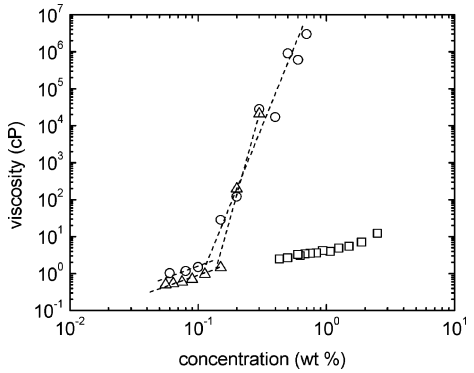

Figure 2. Double-logarithmic plot of zero shear viscosity η as a function of polymer concentration in aqueous solution at pH 3 and 25 °C for (○) MMA_{32}−$DMAEMA_{224}$−MMA_{32}, (△) MMA_{35}−$DMAEMA_{180}$−MMA_{35}, and (□) MMA_{16}-*b*-$DMAEMA_{252}$-*b*-MMA_{16}.

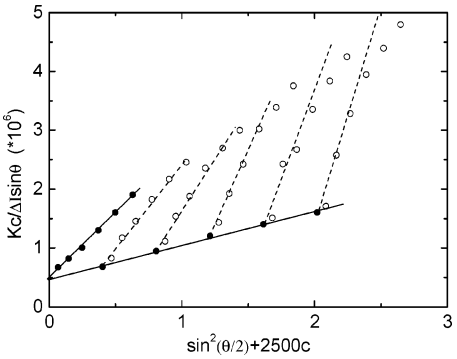

Figure 3. A Zimm plot of the MMA_{32}-*b*-$DMAEMA_{224}$-*b*-MMA_{32} aqueous solutions at pH 3 in the concentration range 0.016−0.1 wt %.

^{1}H NMR was close to the theoretically expected from the comonomer feed ratio during synthesis. The molecular weights of the copolymers were determined by those of the precursor homopolymers and the copolymer composition. All the molecular characteristics of the copolymers have been collected in Table 1.

Hydrogen Ion Titration. The effective p*K*s of the DMAEMA units in all polymers were determined to be around 7.0, in agreement with previous work.[9] The homopolymer (precursor) solution remained optically clear during the titration between pH 2 and 12, while the triblock copolymers precipitated at pH higher than 9.9 (Table 1). Representative hydrogen ion titration curves of the homopolymer and the corresponding copolymer are shown in Figure 1. In the following all the experiments were carried out at pH 3 where the PDMAEMA middle block was fully protonated to ensure the polyelectrolyte character of the associative polymer.

Determination of Gelation Concentrations. It is known that above a certain concentration the associative telechelic polyelectrolytes undergo a hierarchical intermolecular association through hydrophobic attraction of their end-stickers, forming micellar aggregates and a three-dimensional network at elevated concentrations.[5,8]

The critical concentration, c_{gel}, above which a physical gel is formed, macroscopically observed by a rapid increase of the solution viscosity, was determined by steady-state shear viscosity measurements. The concentration dependence of the zero-shear viscosity as a function of concentration for the three associative TP is depicted in Figure 2. c_{gel} was determined at the concentration corresponding to the intersection of the straight lines denoting the onset of a transient infinite network formation. It is obvious that c_{gel} depends on the macromolecular characteristics of the TP. MMA_{32}−$DMAEMA_{224}$−MMA_{32} exhibited a lower c_{gel} than MMA_{35}−$DMAEMA_{180}$−MMA_{35} probably due to the longer mid-block (bridging chains between the hydrophobic PMMA domains). However, in the case of MMA_{16}−$DMAEMA_{252}$−MMA_{16} although it bears the longest mid-block, no gel formation was observed up to $c_p = 3$ wt %. This fact should be attributed to the small length and the nature of the PMMA stickers. It seems that in the concentration range investigated the molecular futures of this TP were not suitable enough to permit the formation of a stable three-dimensional network.

Association Phenomena by Light Scattering. In the following, MMA_{32}−$DMAEMA_{224}$−MMA_{32} was chosen for exploring the association phenomena by using static (SLS) and dynamic light scattering (DLS) experiments. SLS experiments on a series of aqueous solutions at concentrations between 0.016 and 0.100 wt % were carried out, and the obtained Zimm plot is depicted in Figure 3. From the extrapolated zero angle $K_c/\Delta I$ values, an average apparent aggregation number was calculated to be $N_{agg} = 51$. The zero concentration angular dependence of $K_c/\Delta I$ gave an apparent radius of gyration $R_g = 142$ nm. This value is much higher than the contour length of the PDMAEMA polyelectrolyte block (56 nm), suggesting the formation of nonmicellar aggregates. However, as can be observed in Figure 3, the Zimm plot was not regular since the angular dependence changed with concentration. Indeed, the deviation from linear dependence is more and more remarkable, and the initial slope

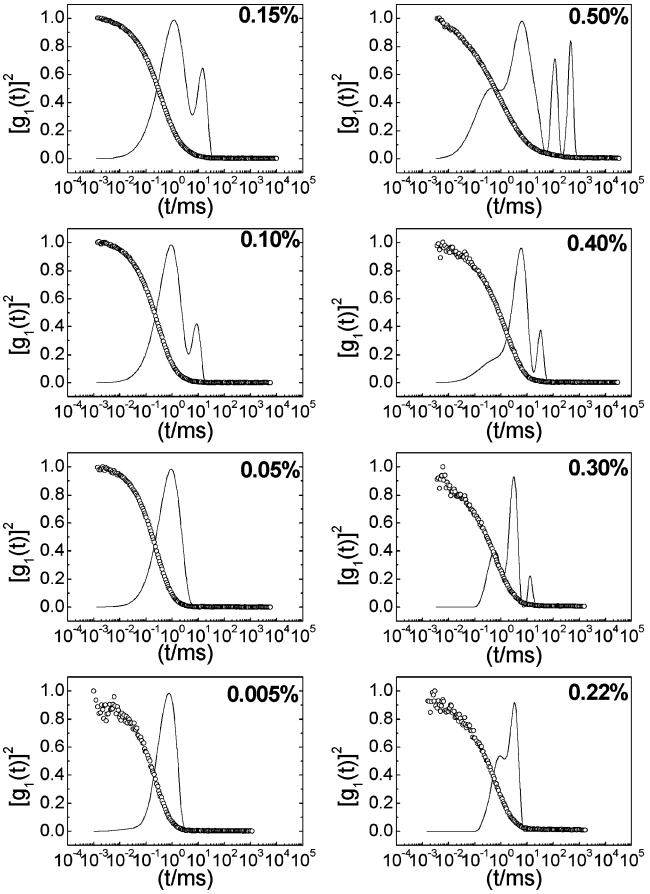

Figure 4. Normalized autocorrelation functions (○) and time relaxation distributions (—) obtained from dynamic light scattering at scattering angle $\theta = 90°$ in aqueous MMA_{32}-*b*-$DMAEMA_{224}$-*b*-MMA_{32} copolymer solutions at pH 3 and several concentrations.

increases as concentration increases, suggesting a progressive enhancement of the polydispersity and the size of the larger aggregates.

DLS was employed to follow the association mechanism below and above c_{gel} in the range from 5×10^{-3} to 0.5 wt %. Characteristic plots of the autocorrelation function and the corresponding inverse Laplace transformation performed by CONTIN are presented in Figure 4. Monomodal distribution of the relaxation times can be observed at low concentrations (5×10^{-3} wt %) below c_{gel}. This relaxation process exhibits diffusive character as evidenced from the q independence of the D_{app}, giving an apparent $R_h = 108$ nm. As the polymer concentration increases, a second slow relaxation mode (second peak) appeared. Hence, the apparent hydrodynamic radius was increased from 108 to 132 nm in the concentration range (5×10^{-3}—0.1 wt %) while the second peak corresponds to R_h of 1200 nm, demonstrating a rapid growth of the aggregates in the vicinity of c_{gel}. As the concentration further increases above c_{gel}, slower relaxation modes appear which should be attributed to the diffusion of the growing aggregates in accordance with very recent findings in a similar telechelic polyelectrolyte system.[16] Simultaneously, the population of the smaller aggregates decreases in favor of bigger ones. Finally, at polymer concentration $c_p = 0.5$ wt %, four relaxation peaks can be distinguished. The slowest relaxation mode could be correlated to the viscoelastic relaxation time of the forming gel phase[17] which coexist with big aggregates according to theoretical predictions.[16,18] The nonergotic behavior characteristic of true gels has not yet been appeared since the three-dimensional infinite network is formed at concentrations higher than 1 wt % polymer as evidenced by oscillatory shear experiments. In Figure 5, the dynamic moduli of MMA_{32}—$DMAEMA_{224}$—MMA_{32} aqueous solutions are depicted as a function of frequency for two different concentrations, 1.8 and 1.2 wt %. The storage modulus G' is higher than the loss modulus G'', and both are independent from frequency exhibiting elastic behavior in accordance with other TP physical gels.[6,8]

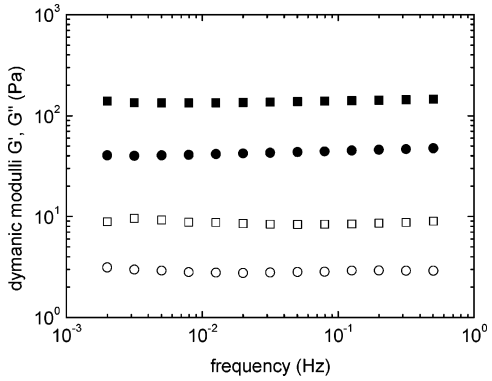

Figure 5. Storage modulus G' (filled symbols) and loss modulus G'' (open symbols) as a function of frequency for MMA_{32}—$DMAEMA_{224}$—MMA_{32} aqueous solution at pH 3, at 1.8 wt % (squares) and 1.2 wt % (circles).

Atomic Force Microscopy. High-resolution atomic force microscopy (AFM) is a powerful technique for the visualization of the conformation of a single macromolecule and the morphology of macromolecular self-assemblies deposited on flat, low-roughness, surfaces from dilute solutions.[19] In this work, we have performed AFM experiments on dry PMMA—PDMAEMA—PMMA molecules deposited on a mica surface from solutions of different concentrations. Previously, we have shown that the so-deposited structures of polar polymer chains (e.g., protonated P2VP) appear to be trapped in the solution conformation due to strong attractions among the positively charged polyelectrolytes and the negatively charged surface (mica).[21] Figure 6 displays AFM images obtained after the deposition from a concentration $c_p = 10^{-4}$ wt %. The polymer molecules appear as 0.5 ± 0.1 nm thick 2D wormlike coils (Figure 6a,b). There are only few chain superpositions (overlaps). Most of the chains are in extended conformations. The latter is consistent with a strong intramolecular electrostatic repulsion in PDMAEMA blocks which are fully protonated at pH 3. The PMMA chain ends appear as collapsed beads (yellow arrows in Figure 6c—e) as expected from their hydrophobic nature. However, in few cases one can observe the onset of association leading to two types of associates. One type results from the end-to-end linear association of two, three, or four macromolecules (Figure 6e). The other type appears as starlike "hairy" loose aggregates where the one end of the TP is located in an irregular hydrophobic core and the other remains as a dangling end (Figure 6c,d). These kinds of aggregates have been predicted by molecular dynamics of semiflexible telechelic polymers.[20] The size of the hydrophobic cores (see cross sections of images in Figure 6c,d) cannot be justified solely from the number of the hydrophobic stickers that participate in the aggregate, implying that nonprotonated DMAEMA units exist in the core in accordance with other findings.[21] This is the first investigation in which both types of association are observed, and they can be attributed to the stretched conformation of the PDMAEMA, arisen from the repulsive electrostatic interactions along the chain, and the relatively short length of PDMAEMA, implying small number of Kuhn segments which prevents looping.

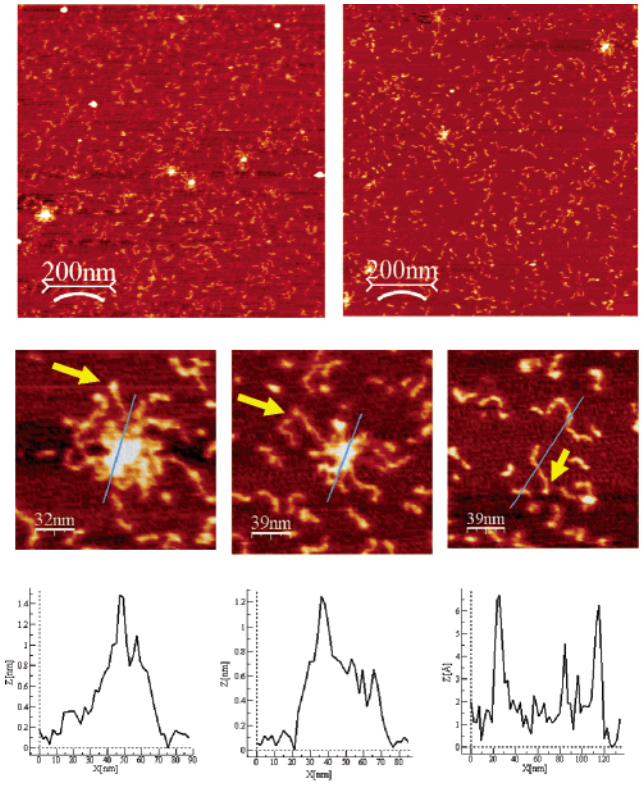

Figure 6. AFM topography images (a, b), associates (details) (c, d, e), and corresponding cross sections of the MMA_{32}-*b*-$DMAEMA_{224}$-*b*-MMA_{32} deposited on mica from low pH aqueous solution and low concentration (10^{-4} wt %). Yellow arrows indicate PMMA hydrophobic beads. The corresponding cross sections for the images c and d demonstrate several time higher thickness for the hydrophobic cores (1.3−1.5 nm) as compared to the thickness of 0.3−0.5 nm for single chains (image e).

To visualize the morphology of the transient network, an AFM experiment was performed on a sample deposited from a polymer solution of concentration slightly above C_{gel}. In Figure 7, the onset of the formation of the expected infinite transient network can clearly be seen. The molecular resolution of this AFM image show for the first time the internal structure of a physical network formed by the association of telechelic polyelectrolytes. The network is formed progressively by the association of irregular finite size clusters (marked by a yellow cycle in Figure 7) in accordance with the results observed by DLS (Figure 4). The formed aggregates look like the finite size clusters predicted by Khokhlov et al.[18] where the bridging chains adopt a stretched conformation (absence of looping chains), interconnecting inner and surface hydrophobic cross-links.

The present findings show a different association mechanism from that reported previously for the S_{35}-*b*-AA_{844}-*b*-$nBMA_9$ heterotelechelic polyelectrolyte in basic aqueous solutions.[8] In the latter case, flowerlike micelles were formed at low concentrations, which were associated through loop-to-bridge transitions, forming bigger micellar aggregates when the concentration increased. The inability of the MMA_{32}-*b*-$DMAEMA_{224}$-*b*-MMA_{32} to form loops seems to be the significantly shorter polyelectrolyte middle block (a few number of Kuhn segments) of the ABA triblock copolymer. Therefore, from the results of the present work it is implied that the morphology of the aggregates formed by the telechelic polyelectrolytes and the way they grow to build the infinite network (gelation mechanism) depend on their molecular characteristics.

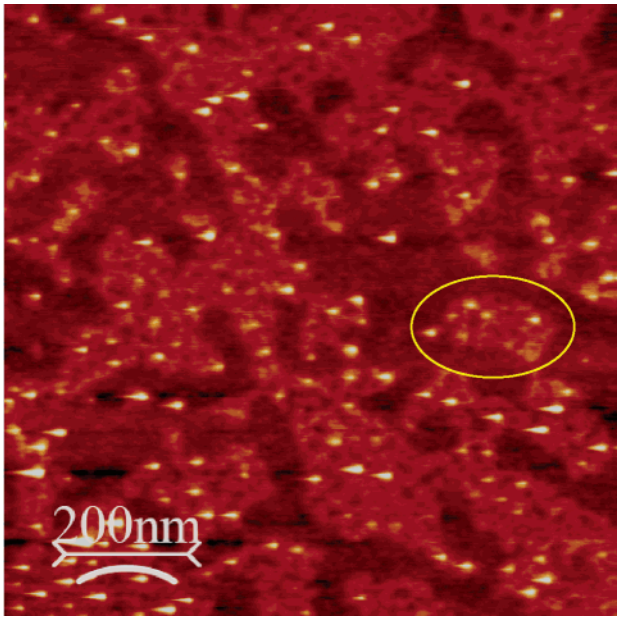

Figure 7. AFM topography images of the MMA_{32}-*b*-$DMAEMA_{224}$-*b*-MMA_{32} deposited on mica from an aqueous solution of concentration 0.25 wt % at pH 3. A finite size cluster (microgel) is marked by the yellow cycle.

Conclusions

The aqueous solution properties of cationic TPs comprising a relatively long poly(dimethylamino)ethyl methacrylate) midblock end-capped by short poly(methyl methacrylate) blocks at both ends (PMMA−PDMAEMA−PMMA) were investigated. The triblock copolymer was synthesized by the GTP method which proceeds at room temperature, an advantage compared to anionic polymerization used so far.[5,7]

In this work, the focus was on the study of the association of the TP in acidic media, while the rheological properties of the formed physical gels will be the subject of a forthcoming paper. The PMMA−PDMAEMA−PMMA copolymers are associated trough the attractive hydrophobic interactions of the PMMA end-blocks as expected. However, novel findings concerning the details of TP self-organization as well as the morphology of the formed aggregates were achieved by using AFM imaging. Two types of associates were observed at very low concentrations and at the onset of association: end-to-end linear associates of a few macromolecules and starlike "hairy" loose aggregates where the one end of TP is located in an irregular hydrophobic core and the other remains as a dangling end (absence of looping chains). By increasing concentration, finite size clusters (microgels) were formed, the size of which changed continuously upon increasing concentration as revealed by DLS. Finally, at sufficiently higher concentrations an infinite transient network is formed, the internal structure of which was visualized for the first time. All the observed structures were mainly attributed to the polyelectrolyte character and the relative small number of Kuhn segments of the central protonated PDMAEMA block.

Acknowledgment. This research was supported through a European Community Marie Curie Fellowship to G.T.G. for his stay at the University of Cyprus. The A. G. Leventis Foundation is gratefully acknowledged for a generous donation, which enabled the purchase of the NMR spectrometer at the University of Cyprus. C.T. and G.T.G. thank the Ministry of Education and Religious Affairs in Greece for the financial support through the Operational Program for Education and Initial Vocational Training on Polymer Science and Technology

of the University of Patras. We also thank Dr. S. Yannopoulos for providing the DLS apparatus. The Clarkson group acknowledges support from the NSF award CTS 0456548.

References and Notes

(1) Winnik, M. A.; Yekta, A. *Curr. Opin. Colloid Interface Sci.* **1997**, *2*, 424.
(2) Berret, J.-F.; Calvet, D. Collet, A.; Viguier, M. *Curr. Opin. Colloid Interface Sci.* **2003**, *8*, 296.
(3) Bhatia, S. R.; Mourchid, A.; Joanicot, M. *Curr. Opin. Colloid Interface Sci.* **2001**, *6*, 471.
(4) Goethals, E. J. *Telechelic Polymers: Synthesis and Applications*; CRC Press: Boca Raton, FL, 1989.
(5) Tsitsilianis, C.; Iliopoulos, I.; Ducouret, G. *Macromolecules* **2000**, *33*, 2936.
(6) Tsitsilianis, C.; Iliopoulos, I. *Macromolecules* **2002**, *35*, 3662.
(7) Tsitsilianis, C.; Katsambas, I.; Sfika, V. *Macromolecules* **2000**, *33*, 9054.
(8) Katsambas, I.; Tsitsilianis, C. *Macromolecules* **2005**, *38*, 1307.
(9) (a) Baines, F. L.; Armes, S. P.; Billingham, N. C.; Tuzar, Z. *Macromolecules* **1966**, *29*, 8151. (b) Triftaridou, A. I.; Vamvakaki, M.; Patrickios, C. S. *Polymer* **2002**, *43*, 2921.
(10) Gohy, J.-F.; Antoun, S.; Jérôme, R. *Macromolecules* **2001**, *34*, 7435.
(11) Vamvakaki, M.; Unali, G.-F.; Bütün, V.; Boucher, S.; Robinson, K. L.; Billingham, N. C.; Armes, S. P. *Macromolecules* **2001**, *34*, 6839.
(12) Triftaridou, A. I.; Hadjiyannakou, S. C.; Vamvakaki, M.; Patrickios, C. S. *Macromolecules* **2002**, *35*, 2506.
(13) Simmons, M. R.; Yamasaki, E. N.; Patrickios, C. S. *Macromolecules* **2000**, *33*, 3176.
(14) Georgiou, T. K.; Vamvakaki, M.; Patrickios, C. S.; Yamasaki, E. N.; Phylactou, L. A. *Biomacromolecules* **2004**, *5*, 2221.
(15) Van Rompaey, E.; Sanders, N.; De Smedt, S. C.; Demeester, J.; Van Craenenbroeck, E.; Engelborghs, Y. *Macromolecules* **2000**, *33*, 8280.
(16) Zaroslov, Y. D.; Fytas, G.; Pitsikalis, M.; Hadjichristidis, N.; Philippova, O. E.; Khokllov, A. R. *Macromol. Chem. Phys.* **2005**, *206*, 173.
(17) Classenieux, C.; Nicolai, T.; Tassin, J.-F.; Durand, D.; Gohy, J.-F.; Jérôme, R. *Macromol. Rapid Commun.* **2001**, *22*, 1216.
(18) Potemkin, I. I.; Vasilevskaya, V. V.; Khokhlov, A. R. *J. Chem. Phys.* **1999**, *111*, 2809−2817.
(19) (a) Minko, S.; Kiriy, A.; Gorodyska, G.; Sheparovych, R.; Lupitskyy, R.; Tsitsilianis, C.; Minko, S.; Stamm, M. Conformation of Polymer Molecules via Atomic Force Microscopy. In *Applications of Scanned Probe Microscopy to Polymers*; Batteas, J. D., Michaels, C. A., Walker, G. C., Eds.; *ACS Symp. Ser.* **2005**, *897*, 207. (b) Gorodyska, A.; Kiriy, A.; Minko, S.; Tsitsilianis, C.; Stamm, M. *Nano Lett.* **2003**, *3*, 365. (c) Kiriy, A.; Gorodyska, G.; Minko, S.; Stamm, M.; Tsitsilianis, C. *Macromolecules* **2003**, *36*, 8704. (d) Roiter, Y.; Minko, S. *J. Am. Chem. Soc.* **2005**, *127*, 15688.
(20) Khalatur, P. G.; Khokhlov, A. R.; Kovalenko, J. N.; Mologin, D. A. *J. Chem. Phys.* **1999**, *110*, 6039.
(21) Tsitsilianis, C.; Voulgaris, D.; Štěpánek, M.; Podhájecká, K.; Procházka, K.; Tuzar, Z.; Brown, W. *Langmuir* **2000**, *16*, 6868.

MA051592E